An Automatic Control System for Measuring Stokes Polarization and Utilizing UV Light Source

Y. Nguyen Le, Yen-Nhi Nguyen, and Thi-Thu-Hien Pham

Abstract Polarization is an elementary property of light waves and has many applications in medicine and health sciences. In this research, an automatic control UV light source Stokes polarimeter system is built using simple and inexpensive optical devices. The optical system includes one UV laser source, three polarizers, two quarter-waveplate, and one optical sensor applying the Mueller-Stokes decomposition for extracting linear birefringence (LB), linear dichroism (LD), circular birefringence (CB), circular dichroism (CD), linear depolarization (L-Dep), and circular depolarization (C-Dep) of a biological sample. The system can measure the intensity of 180 data points then calculate the output Stokes vector of measured samples from 4 inputs polarized lights (i.e., 0°, 45°, 90° of linear polarized lights and right-hand circular). The experimental results showed that the system could automatically measure Stokes parameters of a biological sample with the accuracy at ±5% to compare with the commercial device, Stokes polarimeter. Therefore, the designed system has the benefits not only of extracting the optical parameters of the biological samples but also of improving the accuracy of results by reducing the error effect on the measurement.

Keywords Stokes-Mueller · Stokes polarimeter · Polarized light measurement system

Y. Nguyen Le—Equally contributed.

Y. Nguyen Le · Y.-N. Nguyen · T.-T.-H. Pham (✉)
School of Biomedical Engineering, International University, Ho Chi Minh City 700000, Vietnam
e-mail: ptthien@hcmiu.edu.vn

Vietnam National University Ho Chi Minh City (VNU-HCMC), Ho Chi Minh City 700000, Vietnam

V. Van Toi et al. (eds.), *8th International Conference on the Development of Biomedical Engineering in Vietnam*, IFMBE Proceedings 85,
https://doi.org/10.1007/978-3-030-75506-5_15

1 Introduction

Polarized light has significant potential for applications in the cosmetic industry, chemistry, biology, engineering science, especially medicine [1–5]. Classic applications of the effective parameters include linear birefringence (LB) of the peripapillary retinal nerve fibre layer provides useful information for early glaucoma diagnosis and the complete understanding of scanning laser polarimetry [6, 7]. Moreover, linear birefringence measurement on the myocardium of rat hearts demonstrates the potential application for monitoring regenerative therapy of myocardial infarction [3]. Circular birefringence (CB) measurement of human blood can distinguish the diabetic severity status in patients [2]. Linear dichroism (LD) measurements are useful for characterizing significant properties of molecules that are hidden or support tumour diagnosis [8–10]. In contrast, the circular dichroism (CD) spectrum can be used to analyse and give valuable information about the secondary structure and function of proteins [11–13].

Furthermore, linear depolarization (L-Dep) and circular depolarization (C-Dep) measurements can provide useful knowledge for studying and characterizing turbid media [14]. Many research papers have shown that any polarization state of light can be completely described by four measurable quantities known as Stokes polarization parameters (S0, S1, S2, and S3) [15]. Applying the Mueller matrix method, the proposed system was designed and built for measuring the Stokes polarization parameters from 4 inputs polarized lights (right-hand circular and linear polarized lights in 0°, 45°, 90°) to determine the fundamental optical properties of biological samples including LB, LD, CB, CD, L-Dep and C-Dep [16]. In this research, an automatic control UV laser- Stokes polarimeter system was built to develop a medical device capable of detecting specific diseases, especially tumour or cancer at their early stages.

2 Methods

2.1 Methodology

Based on the analytical technique of Pham and Lo [17, 18], we design an automatic control system for measuring the Stokes parameters of biomedical samples. This control system can determine the optical properties of samples. A rotating half-wave plate will produce various orientations of linearly polarized light. The polarizing element was placed in a rotatable mount during the measurements and then inserted between the light source and the analyser. By applying Stokes polarimetry and Mueller matrix decomposition method [19], the optical parameters were extracted namely linear birefringence (LB), circular birefringence (CB), linear dichroism (LD), circular dichroism (CD), linear depolarization (L-Dep), and circular depolarization (C-Dep). The automatic control system of Stokes polarimeter is shown in Fig. 1.

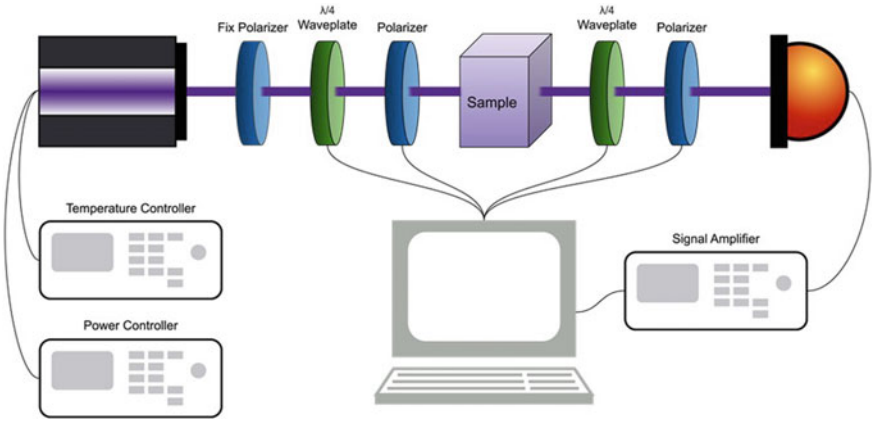

Fig. 1 Schematic illustration of the model of the automatic control UV light—Stokes polarimeter

The system includes a Laser diode source (LDM 785, Co. Thorlabs) with the wavelength of 375 nm firstly generate the light source to a fixed linearly vertical polarizer (LPUV050-MP2, Thorlabs Co.) to normalize and filter the light source, the power controller (LDC200C, Thorlabs Co.) and temperature controller (TEC200C, Thorlabs Co.) were utilized to control the temperature of the laser. Then, the polarization state generator (PSG) with a rotating quarter-wave plate (AQWP05M, Co. Thorlabs) and a rotating linear polarizer (LPUV050-MP2, Thorlabs Co.) generates two circular polarized lights (LH and RH) and four linear polarized lights at 0°, 45°, 90°, 135°. The generated lights interact with the sample and reach the polarization state analyser (PSA) part including another rotating quarter-wave plate (AQWP05M, Co. Thorlabs), a fixed vertical polarizer (LPUV050-MP2, Thorlabs Co.) and a biased Gallium Phosphide photodetector (DET25K/M-GaP Detector, 150–550 nm, Co. Thorlabs) for measuring the light intensity and output the photocurrent. This current was amplified by a photodiode amplifier (PDA200C, Thorlabs Co.) before reading by a computer. Based on the rotating quarter-wave plate polarimeter Stokes method, the rotating quarter-wave plate in the PSA rotates from 0° to 180° and 180 data sample points were obtained by the detector. It will rotate with the steps of 1° ($\theta n + 1 - \theta n = 180/180 = 1°$). Therefore, the angles of rotation are: $\theta 1 = 0°$, $\theta 2 = 1°$, $\theta 3 = 2°$ … $\theta 179 = 178°$, $\theta 180 = 179°$; with every angle of rotation the system reads the analogue signal. Lastly, for each polarized light, 180 measurement data points will be converted to digital signals and computed to Stokes vectors by the equations:

$$\mathrm{A} = \frac{2}{\mathrm{N}} \sum_{\mathrm{n}=1}^{\mathrm{N}} \mathrm{In}|\mathrm{B} = \frac{4}{\mathrm{N}} \sum_{\mathrm{n}=1}^{\mathrm{N}} \mathrm{I_n} \sin 2\theta_\mathrm{n} \tag{1}$$

$$C = \frac{4}{N} \sum_{n=1}^{N} I_n \cos 4\theta_\mathrm{n}|\mathrm{D} = \frac{4}{\mathrm{N}} \sum_{\mathrm{n}=1}^{\mathrm{N}} \mathrm{I_n} \sin 2\theta_\mathrm{n} \tag{2}$$

$$S_0 = A - C, \quad S_1 = 2C, \quad S_2 = 2D, \quad S_3 = B \tag{3}$$

Additionally, the Degree of Polarization, Azimuth and Ellipticity of each data point was calculated the following equations:

$$\text{DOP} = \frac{\sqrt{S_1^2 + S_2^2 + S_3^2}}{S_0} \tag{4}$$

$$\text{Azimuth} = 90^\circ - \frac{\tan^{-1}\left(\frac{S_1}{S_2}\right)}{2} \tag{5}$$

$$\text{Ellipticity} = \frac{\tan^{-1}\left(\frac{S_3}{\sqrt{S_1^2+S_2^2}}\right)}{2} \tag{6}$$

A graphical user interface application was designed to control the system and display the output conveniently algorithm written in MATLAB by Thi-Thu-Hien Pham was used to extract the output results, i.e., Stokes vectors, the Degree of Polarization, Azimuth and Ellipticity of the sample. Brief processes of MATLAB program were shown in Fig. 2.

The Stokes parameters were processed in MATLAB program by applying the Mueller matrix decomposition for extracting nine effective optical parameters including orientation angle of the fast axis of LB, linear birefringence of LB, optical rotation of CB, orientation angle of LD, linear dichroism of LD, circular dichroism of CD, linear depolarization, and circular depolarization.

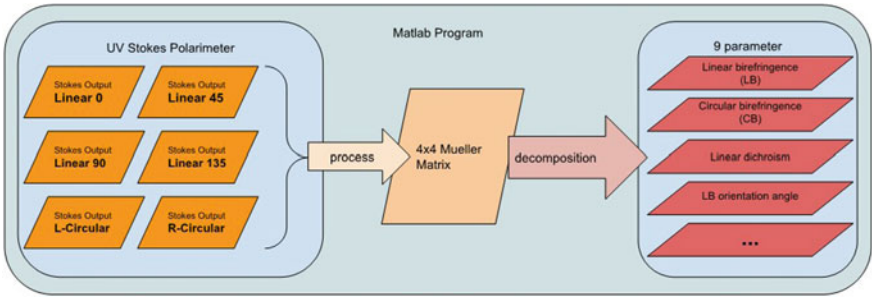

Fig. 2 The processing pipeline of the algorithm written in MATLAB

2.2 Hardware Design

The hardware of the system is designed in two main parts. The first part is an optic mounting, including the gear part controlled by a stepper motor. The holder was linking with the gear part using a magnet and the optic holder to secure the positions of the plates without damaging. With the magnet, the optic mounting can easily disassemble its components or change the tilt angle of the optic. The second part is the rotating optic module, which was created to control the optic angle, including two blocks fixed two stepper motors, which were placed in symmetry and connected with the optic mount by a belt drive.

All optic mounts and the rotating optic module were designed using Autodesk Fusion 360 and printed by 3D printers.

2.3 Firmware and Software Development

Targeting to an automatic control system, the firmware and software were developed to have the most ability to do measurement with less control from the user. The position of the fast axis of each optic was saved in Electrically Erasable Programmable Read-Only Memory of microcontroller to reduce the calibration of the system. The microcontroller was used to control hardware components, read and convert the analogue signal from the sensor. The software is designed by using C Sharp, giving it the ability to fast process and controlling the system. The flowchart of the software algorithm to control the system for generating six polarized light states and analysing the output light after going through the sample, as illustrated in Fig. 3.

3 Results and Discussion

3.1 Designed Hardware

Optic Mounting

In Fig. 4, the optic mount was designed to secure optical components without damaging the optic and controlled by a stepper motor. Thanks to the design of optic mounting with magnets, the optical elements are easily removed or replaced. The tilt angle of optical can be changed from -20 to $20°$.

The gear part operated by a stepper motor was designed to link with the holder by magnets. This part has a home point for marking the optical angle. The optic holder was designed for the insertion of the plates, linear polarizer mount LPUV050-MP2 and quarter-wave plate AQWP05M from Thorlabs Co., as shown in Fig. 5.

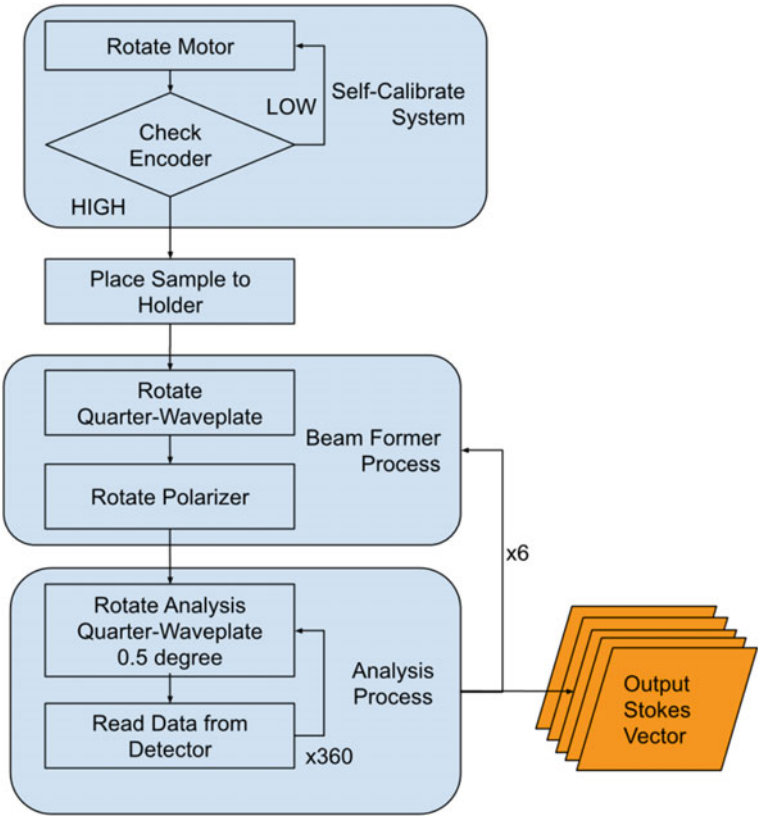

Fig. 3 The flow chart of the automatic Stokes measurement system

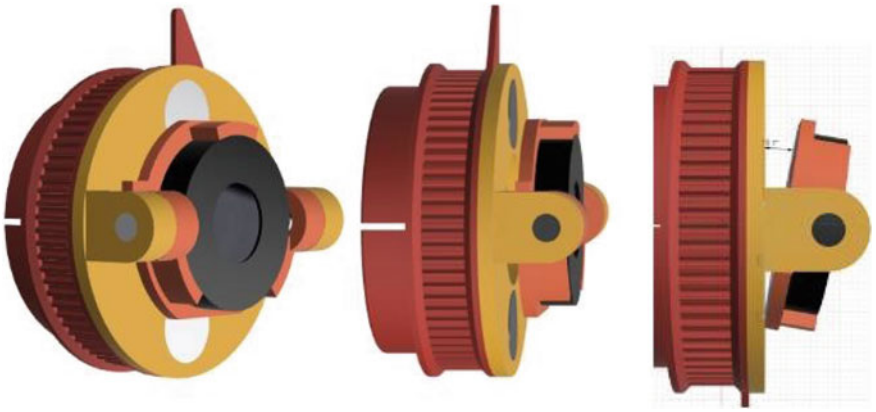

Fig. 4 The design of the optic mounting which was designed allowing the user to change the tilt angle of retarder from −20 to 20° with removable characteristic due to magnet linking

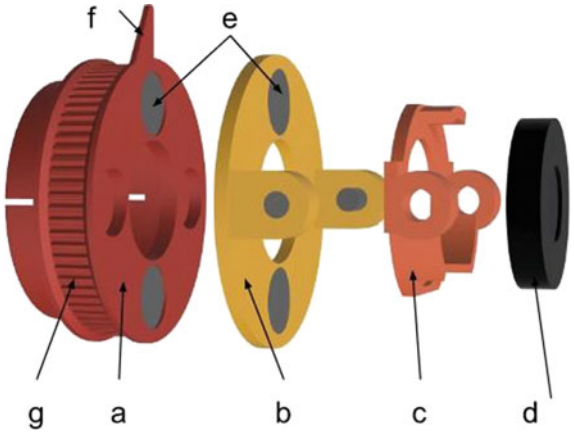

Fig. 5 **a** The gear part with magnets; **b** The holder with magnets to link with (**a**); **c** The optic holder part, designed to tilt the optic from −20 to 20°; **d** The optic; **e** Magnets; **f** The home point to mark the angle of optic; **g** Gear teeth

According to Meadowlark Optics Incorporated [20], the source errors, namely wavelength, angle of incidence, thermal, and the presence of multiple reflections can change the retardation. To avoid inaccurate retardance error, the optic mounting is designed to be able to alter the tilt angle of the optic. The equation calculates the retardance:

$$\delta = (n_e - n_o)\frac{t}{\lambda} = \frac{ßt}{\lambda} \tag{7}$$

where t is the thickness of optic and λ is the wavelength of light, n_e is the extraordinary index, n_o is the ordinary index, ß is a birefringence. This equation proves that wavelength has a significant impact on retardation. The angle of incidence is another source error because it can change the extraordinary index. Retardation can change by temperature since it can change the thickness of the retarder and the birefringence of the material. The retardation is also affected by the presence of multiple reflections caused by the similarity of the coherence length of the light source and the thickness of the retarder.

Therefore, the optic mounting is designed to have the capability to change the tilt angle of the retarder from −20 to 20° for optimizing quarter-wave of retardance for each wavelength.

Optic Rotation Module

The block was designed to fit the stepper motor to control the polarizer lens angle. The stepper motor-operated the optic mounting through belt drives. The system has two optic rotation modules; each module has two motors and two optic holders placed in symmetry. This symmetry design was optimized to reduce the length of the light path or distance between two optics, the unbalancing of the mass balance of the module

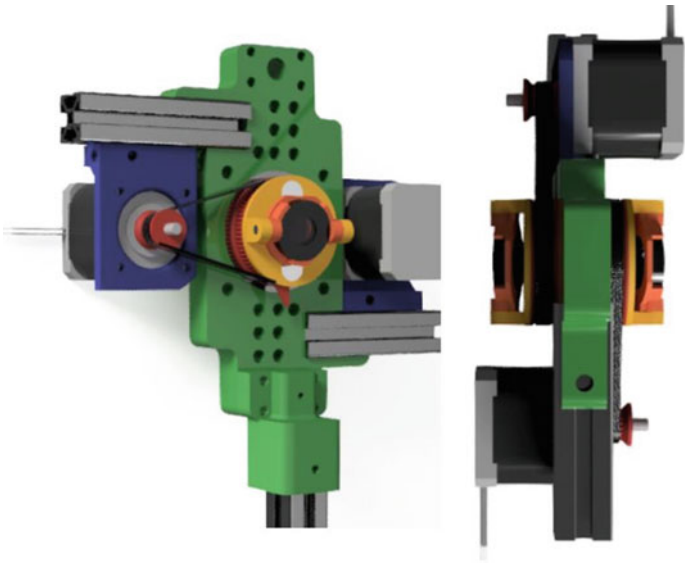

Fig. 6 Design of the optic rotation module using Autodesk Fusion CAD. The module was designed to rotate the optic holder, consisting of two motors and two optic holders placed in symmetry

was also reduced. The optic rotation module was designed as following shown in Fig. 6.

The design of the automatic measurement of the UV Laser system was shown in Fig. 7. This design consists of 2 main parts. The first part is PSG including a Laser diode source and a first module attaching a rotating quarter-wave plate with a rotating linear polarizer. This part served as the generator of 6 inputs polarized lights. To calibrate the light source, a fixed linearly vertical polarizer is inserted before the first module. The second part is PSA consisting of a second module, which has a rotating quarter-wave plate, a fixed vertical polarizer, and a photodetector for measuring the analogue signals and calculating the Stokes parameters.

The light with the wavelength of 375 nm is firstly created by the light source, passes through a rotating quarter-wave plate and a rotating linear polarizer to produce sequentially six polarized light (two circular polarized lights and four linear polarized light). Subsequently, these lights interact with the sample, followed by reaching another rotating quarter-wave plate, a fixed vertical polarizer, and a photodetector for obtaining the analogue signal and calculating the intensity.

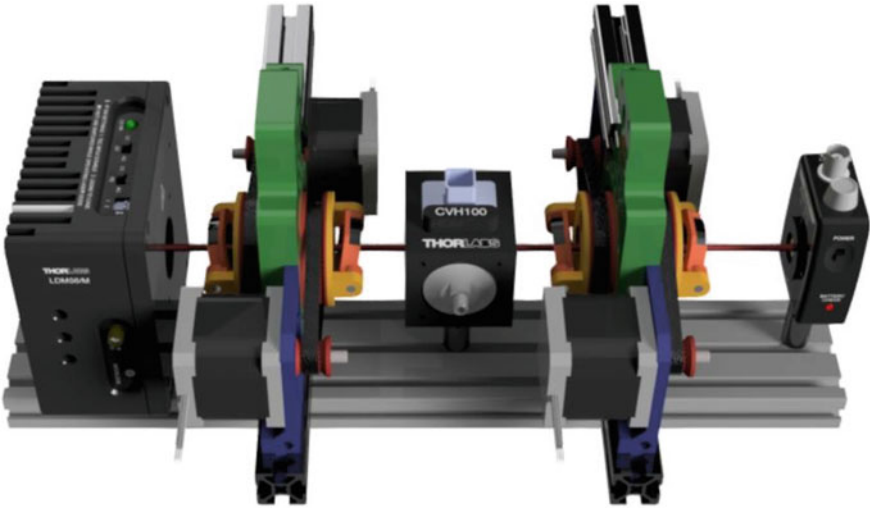

Fig. 7 The design of the system in autodesk fusion CAD. The system is designed into two main parts. The first part is the polarization state generator (PSG) including a laser diode source and a first optic rotation module for generating six inputs polarized lights. The second part is the polarization state analyser (PSA) including a second module and a photodetector for receiving the analogue signal and calculating the Stokes vectors

3.2 Validation for Accuracy of the System

Accuracy of Optic Rotation and Photodetector

A first experiment that is used to validate the accuracy of the motor and photodetector was set up to measure the light intensity of UV laser through a fixed polarizer and rotate another polarizer. Hypothetically, the output intensity recorded will be calculated by $I = I_o*(\cos(a))^2$, where (a) is the angle formed by the polarizer and the light axis; I_o is the intensity when the polarizer is parallel with the light axis. The error of the system was determined by subtracting the measured values to expected values, as shown in Eq. (8):

$$\%error = \left| \frac{Measured\ values - Expected\ values}{Expected\ values} \right| * 100\% \tag{8}$$

In our experiment, the measured data were compared with the expected values. The results of the system are well fitted with the mathematical assumption, as shown in Fig. 8. The accuracy of the motor and the light detector were perfectly validated in this experiment with the error is 0.25% of reading.

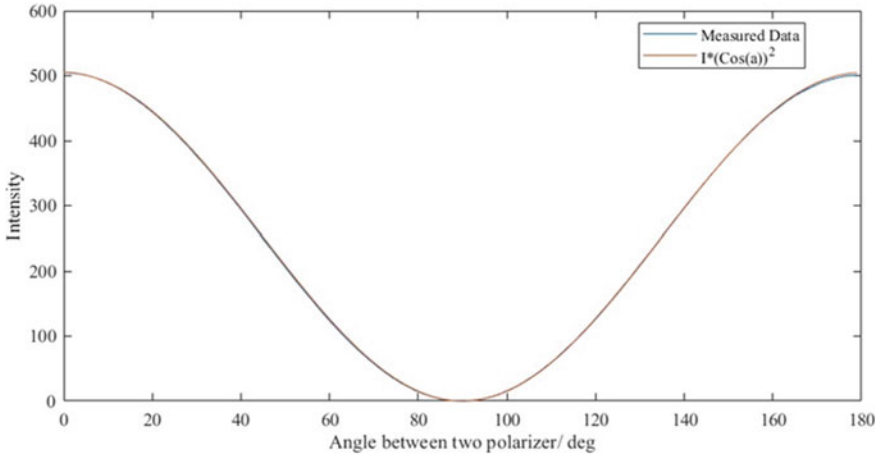

Fig. 8 The comparison of the results of the designed system and the expected values

The Output of Polarization State Generator (PSG)

The outcomes of the generated light from PSG, including Stokes vector, the degree of polarization, azimuth and ellipticity were measured and shown in Table 1.

The generated lights had an error from −0.2% to 1.1% about DOP satisfied the project goal to have the error below 5%. An experiment to extract the properties of the half-wave plate with generated lights was done and reported in the below part of the paper. The result was very good but can improve in the future.

Table 1 The outcomes of the generated polarized lights from PSG

	S_0	S_1	S_2	S_3	Azimuth	Ellipticity	Degree of Polarization
Linearly polarized 0°	1	1.007	0.009	−0.026	45.26	−0.73	100.8
Linearly polarized 45°	1	−0.027	1.011	−0.024	90.76	−0.66	101.1
Linearly polarized 90°	1	−0.998	−0.021	−0.017	45.59	−0.47	99.8
Linearly polarized 135°	1	0.003	−0.988	−0.011	90.76	−0.67	101.1
Left-hand circularly polarized	1	−0.059	0.007	−1	131.71	−44.91	100.2
Right-hand circularly polarized	1	0.039	0.029	0.997	63.23	43.60	99.8

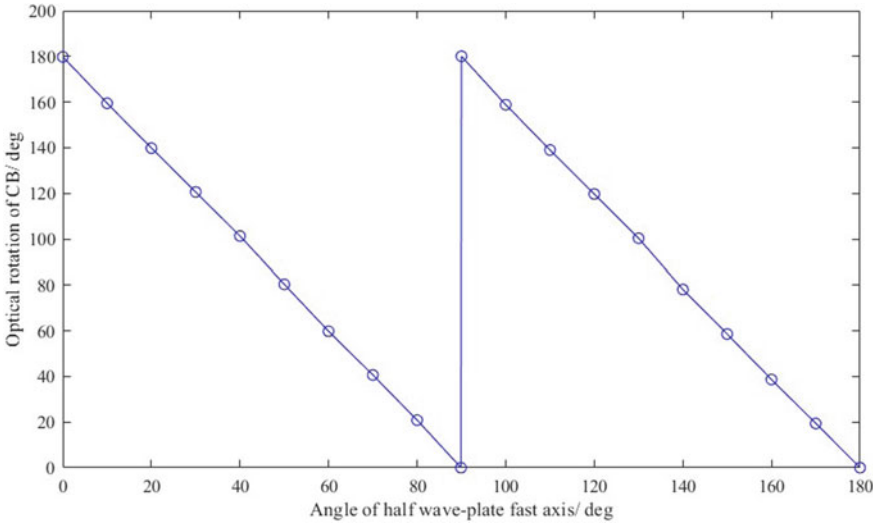

Fig. 9 The extracted optical rotation of CB property of a rotating half-wave plate when it rotated from 0° to 180°

Decomposition of Rotating Half Waveplate

To validate the accuracy of the motor and photodetector, a standard Achromatic Half-Wave Plate (AHWP05M-340, Thorlabs Co.) was positioned at the sample location (see Fig. 1) and rotated from 0 to 180°. After that, through extracting the LB, LD and CB properties of the half-wave plate, the accuracy was assessed. The results are illustrated in Fig. 9.

For each rotation of the half-wave plate, the optical rotation of CB decreases 10°, which is equal to the increasing angle of the half-wave plate, followed by starting a new cycle at the next 90° of the optic.

4 Conclusion

In conclusion, the system was designed, built and tested for automatically measuring the Mueller matrix of the samples with error ±0.25% for reading data. Thanks to the Stokes-Mueller matrix decomposition, nine effective parameters in LB, LD, CB, CD, L-Dep or C-Dep were extracted for investigating the optical properties of the sample. For future works, more rigorous experiments with biological samples and chemical compounds need setting up to characterize their optical properties that could be obscured by using other methods or compare the differences between the healthy and abnormal tissues which is contributed to the cancer diagnosis. This system not only minimizes the time consumption and reduces the errors by users in experiments. It is

a promising device for diseases diagnosis and monitoring development or supporting tumour detection in the future.

Acknowledgements This research is funded by the Vietnam National Foundation for Science and Technology Development (NAFOSTED) under grant number 103.03-2019.381.

Conflicts of Interest The authors have no conflict of interest to declare.

References

1. Wu PJ, Walsh JT (2006) Stokes polarimetry imaging of rat tail tissue in a turbid medium: degree of linear polarization image maps using incident linearly polarized light. J Biomed Opt 11(1):14031
2. Sun P, Ma Y, Liu W, Yang Q, Jia Q (2014) Mueller matrix decomposition for determination of optical rotation of glucose molecules in turbid media. J Biomed Opt 19(4):46015
3. Wood MF, Ghosh N, Wallenburg MA, Li SH, Weisel RD (2010) Polarization birefringence measurements for characterizing the myocardium, including healthy, infarcted, and stem-cell-regenerated tissues. J Biomed Opt 15:047009
4. Bargo PR, Prahl SA, Goodell TT, Sleven RA, Koval G, Blair G, Jacques SL (2005) In vivo determination of optical properties of normal and tumor tissue with white light reflectance and an empirical light transport model during endoscopy. J Biomed Opt 10:034018-1–034018-15
5. Moffitt T, Chen YC, Prahl SA (2006) Preparation and characterization of polyurethane optical phantoms. J Biomed Opt 11:041103-1–041103-10
6. Huang X-R, Knighton RW (2002) Linear birefringence of the retinal nerve fiber layer measured in vitro with a multispectral imaging micropolarimeter. J Biomed Opt 7(2):199–204
7. Huang X-R, Bagga H, Greenfield DS, Knighton RW (2004) Variation of peripapillary retinal nerve fiber layer birefringence in normal human subjects. Invest Ophthalmol Vis Sci 45(9):30733080
8. Liu GL, Li Y, Cameron BD (2002) Polarization-based optical imaging and processing techniques with application to the cancer diagnostics. In: Proceedings SPIE, San Jose, CA, USA, pp 208–220
9. Wemyss AM, Razmkhah K, Chmel NP, Rodger A (2018) Fluorescence detected linear dichroism of small molecules oriented on polyethylene film
10. Nordén B (1978) Applications of linear dichroism spectroscopy. Appl Spectrosc Rev 14(2):157–248
11. Berova N, Nakanishi K, Woody RW (2000) Circular dichroism: principles and applications. Wiley-VCH, Weinheim
12. Kelly SM, Jess TJ, Price NC (2005) How to study proteins by circular dichroism. Biochim Biophys Acta (BBA) Proteins Proteomics 1751(2):119–139
13. Kelly SM, Price NC (2000) The use of circular dichroism in the investigation of protein structure and function. Curr Protein Pept Sci 1(4):349–384
14. Ghosh N, Wood MF, Vitkin IA (2008) Mueller matrix decomposition for extraction of individual polarization parameters from complex turbid media exhibiting multiple scattering, optical activity, and linear birefringence. J Biomed Opt 13:044036
15. Bickel WS, Bailey WM (1985) Stokes vectors, Mueller matrices, and polarized scattered light. Am J Phys 53(5):468–478
16. Firdous S, Ikram M (2012) Stokes polarimetry for the characterization of biomaterials using liquid crystal variable retarders. In: Proceedings SPIE 2012, vol 6632, p 66320F
17. Pham T-T-H, Lo Y-L (2012) Extraction of effective parameters of anisotropic optical materials using decoupled analytical method. J Biomed Opt 17(2):25006-1–25006-17

18. Pham T-T-H, Lo Y-L (2012) Extraction of effective parameters of turbid media utilizing the Mueller matrix approach: study of glucose sensing. J Biomed Opt 17(9):0970021–09700215
19. Lu SY, Chipman RA (1996) Interpretation of Mueller matrices based on polar decomposition. J Opt Soc Am A 13(5):1106–1113
20. Sources of error in retarders and waveplates. Meadowlark.com